

Atomistic structure of monocrystalline silicon in surface nano-modification

This article has been downloaded from IOPscience. Please scroll down to see the full text article.

2004 Nanotechnology 15 104

(<http://iopscience.iop.org/0957-4484/15/1/020>)

View [the table of contents for this issue](#), or go to the [journal homepage](#) for more

Download details:

IP Address: 129.94.206.86

The article was downloaded on 07/06/2012 at 05:35

Please note that [terms and conditions apply](#).

Atomistic structure of monocrystalline silicon in surface nano-modification

I Zarudi¹, W C D Cheong¹, J Zou² and L C Zhang^{1,3}

¹ School of Aerospace, Mechanical and Mechatronic Engineering, The University of Sydney, NSW 2006, Australia

² Australian Key Centre for Microscopy and Microanalysis and Electron Microscope Unit, The University of Sydney, NSW 2006, Australia

Received 17 April 2003, in final form 12 August 2003

Published 14 November 2003

Online at stacks.iop.org/Nano/15/104 (DOI: 10.1088/0957-4484/15/1/020)

Abstract

This paper presents both experimental and theoretical studies on the atomic structure changes of monocrystalline silicon brought about by surface nano-modification. The experiment revealed amorphous transformations with boundaries featuring faceting along $\{111\}$ planes near the sample surface, which were altered to a random nature at the bottom of the transformation zone. The deformation outside the zone was minor near the surface, but advanced to heavy bending, extensive dislocations and plane shifting in the depth of the samples. Theoretical analysis closely reproduced this deformation, highlighting some scaling effects.

(Some figures in this article are in colour only in the electronic version)

1. Introduction

The fabrication of structures with characteristic dimensions approaching nano-scales and even the atomic limit is becoming imperative for information and integrated circuit technology, requiring a profound understanding of the nano/micro-surface processing mechanisms involved [1].

So far, in-depth understanding of atomic surface modification in monocrystalline silicon has come mainly from molecular dynamics analysis [2–4]. It was found that amorphous transformation was the main deformation in silicon when the surface modification unit was at the atomic scale and the stress criterion for this type of deformation was worked out [2]. Relevant experimental studies at the micro/nano-scale [5–9] showed more complex structures in the transformation zone. Micro-indentations with low indentation loads (spherical indenter) initiated amorphous zones of nearly spherical shape [10]. However, when the indentation load increased, the transformation zone changed to a conical shape and featured a crystalline structure of R8/BC8 phases [10]. It was argued that the zone structure in indentation could also be altered by the unloading rate, with fast unloading promoting an amorphous transformation and slow unloading leading to enhanced crystalline decomposition [11–13]. Two- or three-body sliding processes also confirmed the amorphous phase transformation [5, 9]. Nevertheless, various silicon

polymorphs were found [13]. In addition, subsurface zones were characterized by a damaged layer composed of micro-cracks and a high dislocation density. The depth of the damaged layer was progressively reduced with decrease of the material removal scale [6]. Limited studies on the changes in atomistic structure by means of high-resolution electron microscopy (HREM) confirmed the amorphous transformation [7, 10, 14]. However, so far no details on the amorphous–crystalline boundary and nano-deformation in surface nano-modification have been ascertained. In addition, the correspondence between experiment and theory was problematic due to significant differences in scaling.

In this paper we have succeeded in further reducing the scaling gap between theoretical and experimental analysis in ultra-precision polishing (three-body sliding) and made possible a correlation between them.

2. Method

2.1. Experiment

All experiments were conducted on the (100) surfaces of monocrystalline silicon components. Surface nano-modification was performed on a PM5 Auto-Lap precision surface modification machine (Logitech) in a closed environment with nitrogen to minimize possible surface oxidation. The abrasive used was α -Al₂O₃ with an average radius of 25 nm. In the

³ Author to whom any correspondence should be addressed.

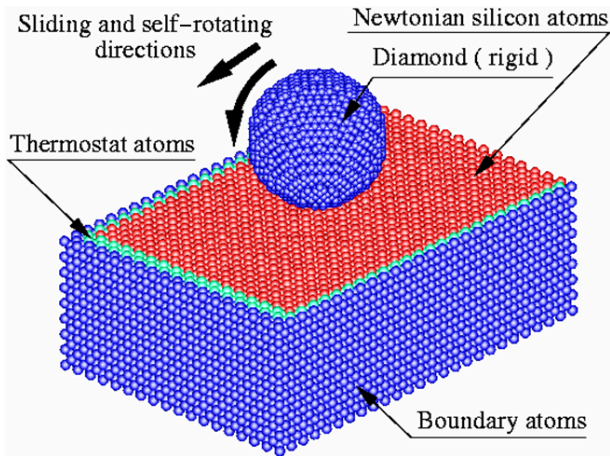


Figure 1. The model for molecular dynamics analysis.

experiment, abrasives were rolled along the silicon surface under a nominal surface pressure of 42 kPa and a table rotation speed of 52 rpm. The nano-scratches on the surface were then studied with HREM in cross-sectional view.

Conventional TEM studies were carried out in a Philips CM12 transmission electron microscope, operating at 120 kV. The HREM investigations were performed in a JEOL JEM-3000F transmission electron microscope, operating at 300 kV.

The $\langle 110 \rangle$ cross-section TEM specimens were prepared using a tripod [15], in which the material removal was continuously monitored and the sample position with respect to the tripod was adjusted during the mechanical thinning. Ion-beam thinning was carried out to provide a sufficiently thin area for the TEM investigations.

2.2. Modelling

The molecular dynamics method enables one to understand the mechanism bringing about the nano-structural change in silicon and hence provide theoretical evidence for the corresponding experimental findings. The method also allows for the simulation of the phase transition at the atomistic scale. The atoms are placed in perfect positions at the beginning, and the resulting structures depend only on the thermomechanical conditions and the interaction forces between atoms, defined by a potential function.

Fundamentally the molecular dynamics analysis involves calculating the phase-space trajectories of each individual atom based on its interaction with the other atoms in accordance with Newtonian dynamics. The phase-space trajectory illustrates the motion of a particle by describing its position in Cartesian coordinates and its momentum. Once the phase-space trajectory is generated it serves as raw data for obtaining time averages of properties.

Figure 1 shows a model of the specimen of silicon monocrystal and a diamond abrasive. The spherical diamond abrasive has a radius of 2.14 nm. The dimension of the control volume of the silicon specimen is made sufficiently large (6.5 nm \times 10.3 nm \times 10.3 nm) to eliminate boundary effects. This is done by ensuring that atomic displacements due to the indentation are effectively insignificant near the boundary of the model.

The maximum penetration depth of the abrasives is 2 nm. To restrict the motion of the specimen, layers of boundary atoms that are fixed to space are used to contain the Newtonian atoms with the exception of the top (100) surface that is exposed to the abrasive. Thermostat atoms are also used to ensure reasonable outward heat conduction away from the control volume. To simulate the machining process under room temperature conditions, the silicon atoms were arranged in a perfect diamond cubic structure with lattice parameters equal to their equilibrium values at an ambient temperature of 23 °C by scaling their velocities at every time step. At the start of the simulation, the model is allowed to relax from its artificially assigned initial conditions to its natural equilibrium status consistent with the environmental temperature of 23 °C. The workpiece is made up of 28 773 atoms and the abrasive is made up of 3636 atoms. The speed of sliding is 200 m s⁻¹.

Before carrying out the molecular dynamics simulation on the surface modification of silicon it is critical to be sure that the potential function used gives a reliable result for the simulation. From our extensive experience [2, 16, 17] we have chosen the Tersoff potential [18] to describe the interactions between the silicon atoms, while the interaction between the silicon atoms and those of the diamond abrasive is described by the Morse potential [19, 20]. In addition, it was ensured that the chosen Tersoff potential is applicable to the modelling of the different phases of silicon before and after the transformation. Based on empirical data, Tersoff [18] showed that the potential is able to model silicon in its diamond cubic and its metallic β -Sn phase with sufficient accuracy and stability.

Another critical issue in the molecular dynamics analysis is the appropriate selection of the time step for the numerical integration of the equations of motion of individual atoms. Too small a time step requires a huge computational cost but too large a time step brings about unreliable results. A suitable time step should be less than 10% of the vibration period of an atom. Hence the optimum time step is dependent on both the specific material and the potential function used.

With the Tersoff potential, an individual atom of silicon or diamond can be forced to move in a direction to show the corresponding stiffness k , so that the period of vibration of the atom in the direction T can be determined by $T = 2\pi(m/k)^{1/2}$, where m is the mass of the atom. A comparison between molecular dynamics simulation using the Tersoff potential with experimental measurements shows that a time step of 1.0 fs for diamond and 2.5 fs for silicon will provide sufficiently accurate integration.

3. Results and discussion

3.1. HREM

Figure 2 shows the diffraction contrast images of a cross section of nano-scratches created by a rolling abrasive. It demonstrates the morphology and microstructure of the transformation zone. The diffraction pattern is inserted to indicate the nature of the material inside the transformation zone.

It is clear that the central region in figure 2 underwent an amorphous phase transformation. The bottom of the amorphous zone has a radius of about 30 nm. The atomistic structure at different locations, indicated by numbers from '1' to '4', will be examined by HREM in more detail.

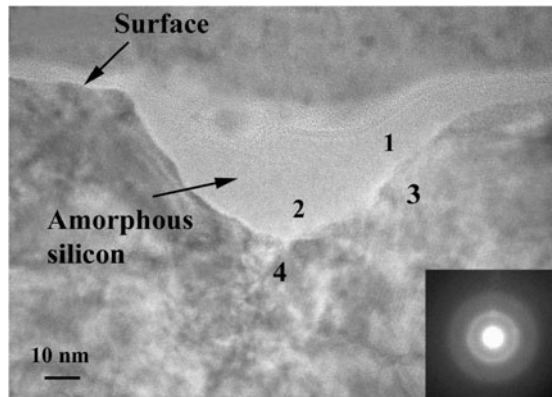


Figure 2. The TEM cross-sectional view of a scratch created in the surface modification (the diffraction pattern of the transformation zone is inserted).

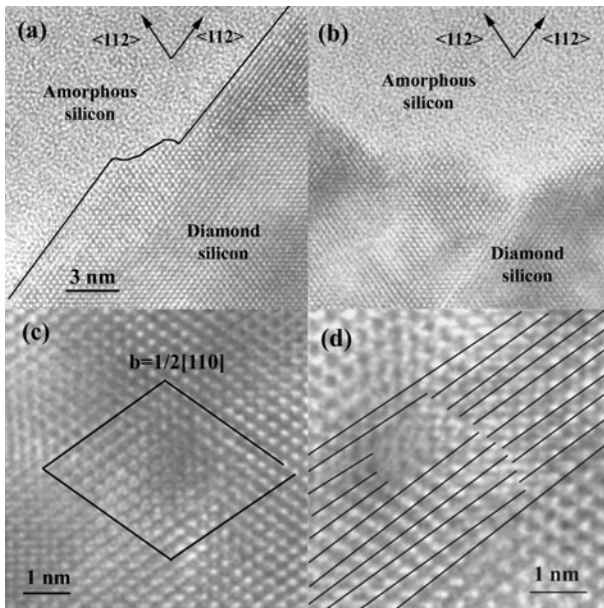


Figure 3. HRTEM images from figure 2. (a) Boundary 1–3. Note that the amorphous phase boundary is going along the $\langle 112 \rangle$ direction and the diamond silicon outside the boundary is almost undisturbed. (b) Boundary 2–4. Note that the amorphous phase boundary does not follow a crystallographic direction. (c), (d) Location ‘4’. Note the dislocation in (c) and the plane shifting in (d) at this location.

Figure 3(a) shows that the boundary of the amorphous transformation zone at location 1–3 features faceting along the $\{111\}$ planes, which is near the sample surface as marked in figure 2. However, the situation becomes quite different at the bottom of the transformation zone (figure 3(b)), location 2–4 in figure 2, where the boundary is irregular.

Outside the transformation zone, the atomic lattice of the material near the surface of the sample, e.g. at location 3, has almost no distortion (figure 3(a)). The internal strains along the $\langle 112 \rangle$ directions were measured to be in a range of $(2-5) \times 10^{-3}$ with an angle distortion between these directions of up to 1° , featuring almost perfect crystallographic arrangements. However, near the bottom of the transformation zone, e.g. at location 4, the plastic deformation of the diamond structure

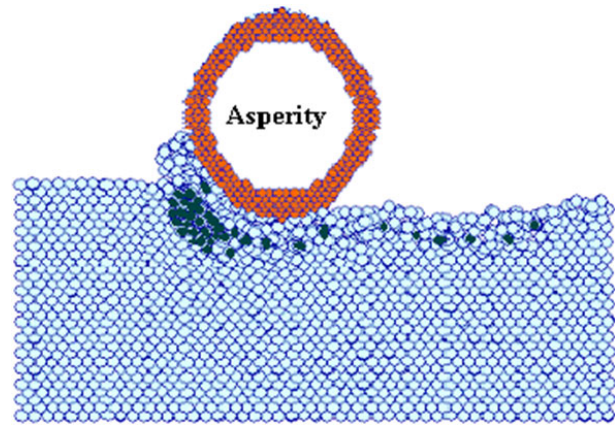


Figure 4. Interaction between a moving abrasive and a bulk silicon (darker circles are β -Sn silicon).

becomes obvious. The measurement of the internal strains in the $\langle 112 \rangle$ directions suggests that it has attained $(16-20) \times 10^{-3}$ with an angle distortion of $4^\circ-7^\circ$. As a result, extensive bending of the atomic planes took place.

Defects such as perfect dislocations (figure 3(c)) and plane shifting (figure 3(d)) have been identified under the bottom of the transformation zone. The initiation of these defects is due to accommodation of a high level of strain by the material. The type of distortion of the crystallographic planes, and especially the sharp rise in the angle variation between $\langle 112 \rangle$ directions, indicates that shear stresses near the bottom of the transformation zone played an important role. The results are aligned well with the theoretical predictions of the stress distribution obtained by the corresponding molecular dynamics simulations [2], which proved there to be a high level of shear stress at the bottom of the transformation zone.

3.2. Molecular dynamics analysis

Molecular dynamics simulations revealed that phase transformation of silicon occurs at the leading edge beneath the abrasive, resulting in the formation of amorphous chips and an amorphous trail along the path traversed by the abrasive. Dislocations are absent at this particular depth of cut. This suggests that the plastic deformation is due to phase transformation. By considering the exact coordinates of the silicon atoms, it is found that the transformation mechanism is similar to that under nano-indentation [21]. Diamond cubic silicon first transforms into its β -Sn silicon and then upon the removal of stresses, the β -silicon transforms into an amorphous phase.

This explains the trail of subsurface amorphous silicon in the damaged zone behind each abrasive particle. The mechanism of phase transformation is reflected in the coordination numbers of atoms near the regions beneath the abrasive particle. It can be seen that a cluster of six-coordinated body-centred tetragonal β -Sn silicon atoms, indicated by darker circles (figure 4), forms near the leading edge beneath the abrasive. Four-coordinated diamond cubic silicon transforms to six-coordinated β -Sn. When the stresses are removed as the abrasive slides past, the atoms transform into an energetically more favourable amorphous form, leaving a layer of subsurface amorphous silicon in its wake.

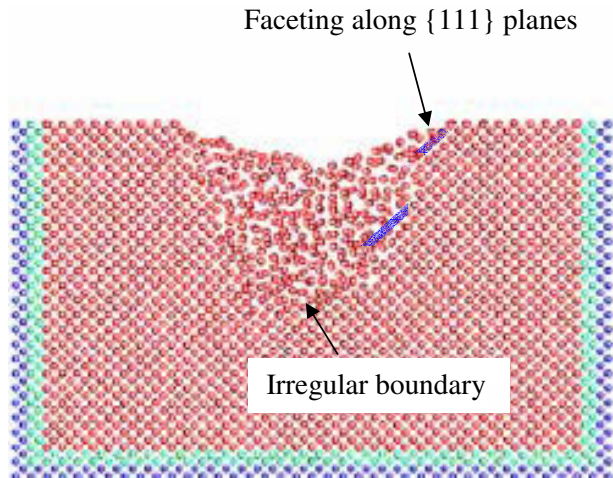


Figure 5. The boundary between the amorphous and the crystalline zone.

The effect of the stress field in surface nano-modification can be understood to a certain degree if the variation of the atomic structures along the boundary of the transformed zone is carefully inspected. At the bottom of the amorphous zone (figure 5) the shape of the crystal–amorphous boundary is irregular, but in all other locations the boundary is mostly regular with faceting along the $\{111\}$ atomic planes. It correlates well with the experimental results presented earlier. No distortion of diamond silicon outside the transformation zone was found.

The comparison of the experimental and theoretical results gives a reasonable correlation, although a scale effect has been identified.

Whilst an amorphous transformation was detected in the present work for both experiment and theory, some details of boundary structure and plastic deformation of bulk silicon are different. As discussed above, both methods (HREM and molecular dynamics simulations) showed that the boundary at the transformation zone presents faceting along the $\{111\}$ planes near the sample surface and becomes irregular near the bottom of the zone. However, in molecular dynamics analysis, the boundary faceting along $\{111\}$ planes extends deeper, reaching almost the bottom of the transformation zone. Faceting of the boundary along $\{111\}$ planes indicates minimization of the boundary energy [22] and also emphasizes the role of the crystallographic anisotropy with scale reduction. On the other hand, inelastic deformation outside the transformation zone was detected in the experiment, but this was not found in the molecular dynamics study. It seems to indicate that the amorphous transformation is more favourable at a finer scale.

It should be noted that no oxidation process was taken into account in the theoretical analysis. However, our previous experimental and theoretical studies [9, 14, 23] showed that there was only shallow surface layer oxidation in surface nano-modification. We believe that we have minimized the oxidation process in our experiment by using the closed environment and inert atmosphere. In addition, the shallow oxidized layer does not affect the shape of the transformation zone or the boundary structure.

4. Conclusions

In summary this study succeeded in bridging the scaling gap between experimental HRTEM studies and theoretical molecular dynamics analysis in surface nano-modification. The following are the main conclusions:

- (1) Interaction between an abrasive particle and silicon leads to multiple phase transformation events. The first phase transformation features the formation of β -Sn silicon during modification loading. An amorphous transformation appears after the particle slides away.
- (2) The boundary of the transformation zone near the modified surface is regular, featuring faceting along $\{111\}$ planes. It becomes irregular at the bottom of the zone.
- (3) There seems to exist a scale effect on the transformation zone boundary. The crystallographic anisotropy plays a more pronounced role at a finer scale. In addition, the inelastic deformation outside the transformation zone, such as dislocations and lattice bending, diminishes with decreasing scale of material removal.

Acknowledgment

The authors wish to thank the Australian Research Council for continuing support of this project.

References

- [1] Yasunaga N 1997 *Proc. Advances in Abrasive Technology* (Singapore: World Scientific) p 18
- [2] Zhang L C and Tanaka H 1998 *Tribol. Int.* **31** 425
- [3] Cheong W C D, Zhang L C and Tanaka H 2001 *Key Eng. Mater.* **196** 31
- [4] Zhang L C, Johnson K L and Cheong W C D 2001 *Tribol. Lett.* **10** 23
- [5] Zarudi I and Zhang L C 1998 *J. Mater. Proc. Tech.* **84** 149
- [6] Zarudi I and Zhang L C 1996 *J. Mater. Sci. Lett.* **15** 586
- [7] Kunz R R *et al* 1996 *J. Mater. Res.* **11** 1228
- [8] Mchedlidze T R, Yonenaga I and Sumino K 1995 *Mater. Sci. Forum* **196–201** 1841
- [9] Zhang L C and Zarudi I 1999 *Wear* **229** 669
- [10] Zarudi I, Zou J and Zhang L C 2003 *Appl. Phys. Lett.* **82** 874
- [11] Bradby J E *et al* 2000 *Appl. Phys. Lett.* **77** 3749
- [12] Domnich V, Gogotsi Y G and Trenary M 2001 *Fundamentals of Nanoindentation and Nanotribology II. Symposium (Boston, MA, USA, November 2000)* vol 649, ed S P Baker, R F Cook, S G Corcoran and N R Moody (Warrendale, PA, USA: Mater. Res. Soc.) p Q8.9.1
- [13] Jeong S N *et al* 2003 *Japan. J. Appl. Phys.* **42** 2773
- [14] Zhang L C and Zarudi I 2001 *Int. J. Mech. Sci.* **43** 1985
- [15] Zarudi I and Zhang L C 1999 *Tribol. Int.* **32** 701
- [16] Tanaka H and Zhang L C 1997 *ISAAT'97: Proc. Advances in Abrasive Technology* (Singapore: World Scientific) p 43
- [17] Zhang L C and Tanaka H 1997 *Wear* **211** 44
- [18] Tersoff J 1989 *J. Phys. Rev.* **39** 5566
- [19] Tanaka H and Zhang L C 1996 *ICPCG-96: Proc. Progress in Cutting and Grinding* (Osaka: Shueisha) p 262
- [20] Zhang L C, Tanaka H and Liu Z 1996 *Proc. 19th Int. Congress of Theoretical and Applied Mechanics—1996* (Kyoto: Japan Scientific Societies Press) p 831
- [21] Cheong W C D and Zhang L C 2000 *Nanotechnology* **11** 173
- [22] Christophersen M *et al* 2001 *J. Electrochem. Soc.* **148** E267
- [23] Mylvaganam K and Zhang L C 2002 *Nanotechnology* **13** 623